A Comparative Study on the Effect of Optical Illumination on $Si_{1-x}Ge_x$ and Si Based DDR IMPATT Diodes at W-Band

A. Acharyya* and J. P. Banerjee*

Abstract: The effect of optical illumination on DC and high frequency performance of $Si_{1-x}Ge_x$ based p^+pnn^+ structured double drift region (DDR) IMPATT device operating at W-Band is investigated and compared with its Silicon counterpart. A double iterative computer simulation method based on drift-diffusion model is used to study the DC and small signal properties of the device under dark condition. The same method is used to study the subsequent modification of the DC and small signal parameters due to optical illumination in both Top Mounted (TM) and Flip Chip (FC) structures where the composition of photocurrent is altered by shining light on the p^+ and n^+ sides of the device respectively through optical widow. Results show that the DC and small signal parameters of both the Si and $Si_{1-x}Ge_x$ based DDR devices are affected significantly due to optical illumination. It is observed that the effect of optical illumination is greater in TM structure of both Si and $Si_{0.5}Ge_{0.5}$ based DDRs compared to FC structure, i.e. electron dominated photo current effect is more prominent than the hole dominated photocurrent in both the devices. But the results significantly indicate that photo-sensitiveness of $Si_{1-x}Ge_x$ based DDR IMPATT is much greater than the Si based DDR IMPATT; which is one of the major findings of this work.

Keywords: Optical Illumination, Flip Chip Structure, Top Mounted Structure, Double Drift Region IMPATT Diode.

1 Introduction

The rapid developments in the process technology of IMPATT device have made possible the fabrication of this device having narrow depletion layer width. IMPATT devices are finding useful application as powerful and efficient sources in various communication systems operating in millimetre-wave and submillimetre-wave bands of frequency. The advantages of millimeter-wave and submillimetre-wave frequencies are many fold such as increased resolution, higher penetrating power of these signals through cloud, dust, fog etc, low power supply voltage and reduced system size [1-3]. Several atmospheric window frequencies are available in the millimetre-wave frequency range (30-300 GHz) such as 35, 94, 140, 220 GHz. This has attracted the attention of researchers working in this area to design and develop IMPATT diodes which can deliver appreciable amount of millimeter wave power of the order of watts at the chosen window frequency. Several theoretical and experimental studies in past few years [4-9] indicate that the modulation of RF properties of IMPATT devices is possible through optical injection. Use of proper opto-sensitive base materials may support this feature of IMPATT utility. In recent time different researchers have proposed various optoelectronic devices based on $Si_{1-x}Ge_x$ [10-12]. Being an alloy of Si (E_g = 1.12 eV) and Ge (E_g = 0.66 eV) the bandgap of $Si_{1-x}Ge_x$ can be varied from 1.12 eV to 0.66 eV by varying the Ge mole fraction x from 0 to 1. The variation of band gap with x for unstrained $Si_{1-x}Ge_x$ is given by $E_g(x) = 1.12 - 0.41x + 0.008x^2$ eV for $x < 0.85$ but $E_g(x) = 1.86 - 1.2x$ eV for $x > 0.85$ at 300 K [13]. The electron and hole mobility of $Si_{1-x}Ge_x$ is calculated from the method described elsewhere [14, 15].

Optical control of the dynamic properties of W-Band IMPATT device may have massive applications in recent time in various fields like advanced radars and space communication systems etc. When a photon (due to optical or other radiation) having energy hν greater than the bandgap energy ($h\nu > E_g$) of the semiconductor base material is absorbed at the n^+ or p^+ side of the $p^+nn^+/n^+np^+/p^+pnn^+$ structured reverse biased IMPATT device, excess electron-hole pairs are created within the active region of the device. This photo-generated excess electron-hole pairs raise the photocurrent and enhance

Iranian Journal of Electrical & Electronic Engineering, 2011.
Paper first received 6 Jan. 2011and in revised form 6 June 2011.
* The Authors are with the Institute of Radiophysics and Electronics, University of Calcutta, 92, APC Road, Kolkata-700009, W. B., India.
E-mail: ari_besu@yahoo.co.in.

the existing thermal leakage current in the IMPATT device. This enhanced leakage current due to optical illumination modifies the avalanche transit time phase delay in the device which causes modification in phase and magnitude of the terminal current in the oscillator circuit. Several interesting results have been found by several researchers in many theoretical and experimental studies in effect of optical illumination on the performance of IMPATT devices based on different semiconductor materials at different frequency bands. These facts have prompted the authors to investigate theoretically the role of external radiation in modulating the high frequency dynamic properties of the $Si_{1-x}Ge_x$ DDR W-Band IMPATT. A double iterative computer simulation method [16-17] based on drift-diffusion model has been used to study the small-signal performance and subsequent modification of the small signal parameters due to optical illumination. The effect of optical illumination on dynamic performance of both $Si_{1-x}Ge_x$ and Si based DDR IMPATT diodes operating at W-Band is investigated and compared. The composition of photocurrent is altered by shining light on the p^+ side (Top Mounted (TM)) and n^+ side (Flip Chip (FC)) of the device through optical windows.

The rest of the paper is organized as follows. Section 2 describes the simulation method to study the DC and small-signal properties of DDR IMPATT device. Simulation results along with the subsequent discussions are given in Section 3. Results are provided in this section in the form of necessary plots and tables. Finally the paper concludes in Section 4.

2 Theory and Simulation Technique

2.1 Design of Doping Profiles

The frequency of operation of an IMPATT diode essentially depends on the transit time of charge carriers to cross the depletion layer of the diode. IMPATT diodes having symmetrical Double drift p^+pnn^+ structure are first designed for operation at 94 GHz window by using computer simulation technique and the transit time formula of Sze and Ryder [18] given by $W_{n,p} = 0.37\ v_{sn,sp}/f_d$; where $W_{n,p}$, $v_{sn,sp}$ and f_d are the total depletion layer width (n or p-side), saturation velocity of electrons/holes and design frequency respectively. Here n^+ and p^+-layers are highly doped substrates and n and p are moderately doped epitaxial layers. The background doping (n and p region doping) is varied in the computer program so that the electric field just punches through the depletion layers ($W_{n,p}$) for a particular value of f_d and a particular biasing current density J_0. Small signal computer analysis is then carried out to obtain the conductance-susceptance or admittance characteristics of the diode. The peak optimum frequency (f_p) for maximum negative conductance can be determined from the admittance characteristics. If the magnitude of f_p differs very much from f_d, the value of J_0 is varied and the computer aided design is repeated until f_p is nearly equal to f_d. The biasing current density is thus fixed from the design calculation as described above.

2.2 Material and Design Parameters

The material parameters like ionization coefficients, saturation drift velocities, mobilities of charge carriers, dielectric constants, bandgaps of the base materials (Si and $Si_{1-x}Ge_x$) used for the analysis are taken from published literatures [13, 19-22]. Design parameters of the devices obtained from simulation are given in Table 1.

2.3 Computer Simulation Techniques

The simulation method consists of three parts: (i) DC analysis, (ii) small-signal analysis, and (iii) simulation technique for studying optical illumination effect. A one-dimensional model of the reverse biased p^+pnn^+ structure shown in Figure 1 has been considered in the present analysis. The following assumptions have been made in the simulation of DC and small-signal behavior of $Si_{1-x}Ge_x$ and Si based DDR IMPATT diodes: (a) the electron and hole velocities have been taken to be saturated and independent of the electric field throughout the space charge layer, (b) the effect of carrier space-charge has been considered, and (c) the effect of carrier diffusion has been neglected.

The simulation method starts with DC analysis described in details elsewhere [16-17]. In this method the computation starts from the field maximum near the metallurgical junction. The distribution of DC electric field and carrier currents in the depletion layer is obtained by the double-iterative computer method, which involves iteration over the magnitude of field maximum (E_m) and its location in the depletion layer. A computer algorithm has been developed for simultaneous numerical solution of Poisson's equation, carrier continuity equations and the space charge equation taking into account the effect of mobile space

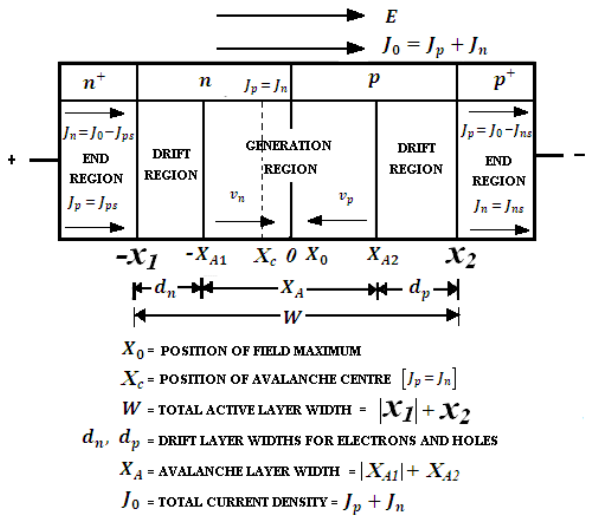

Fig. 1 Different active regions of DDR IMPATT device.

charge and carrier diffusion in order to obtain the electric field profiles and carrier current profiles. The boundary conditions for the electric field at the depletion layer edges are given by,

$$E(-x_1) = 0 \quad \text{and} \quad E(+x_2) = 0 \tag{1}$$

where, $-x_1$ and x_2 define the p^+ and n^+ edges of the depletion layer (origin at the junction). The boundary conditions for normalized current density $P(x) = (J_p(x) - J_n(x))/J_0$ (where, J_p = hole current density, J_n = electron current density) at the edges are given by,

$$P(-x_1) = \left(\frac{2}{M_p} - 1\right) \text{ and } \quad P(+x_2) = \left(1 - \frac{2}{M_n}\right) \tag{2}$$

The necessary device equations have been simultaneously solved [17] satisfying the appropriate boundary conditions mentioned in (1) and (2). The field dependence of electron and hole ionization rates [13, 20] (α_n and α_p) and saturated drift velocities [19, 21-22] of electron (v_{sn}) and holes (v_{sp}) at 300 K are used in the computation for the profiles of electric field and carrier currents. The conversion efficiency is calculated from the semi quantitative formula [25],

$$\eta(\%) = \frac{2m}{\pi} \times \frac{V_D}{V_B} \tag{3}$$

where, V_D = Voltage drop across the drift region, V_B = Breakdown voltage and m = ½.

Avalanche breakdown occurs in the junction when the electric field is large enough such that the charge multiplication factors (M_n, M_p) become infinite. Again, the breakdown voltage is calculated by integrating the spatial field profile over the total depletion layer width, i.e.

$$V_B = \int_{-x_1}^{x_2} E(x)\,dx \tag{4}$$

The high-frequency analysis of Si DDR IMPATT diode provides insight into its high frequency performance. The range of frequencies exhibiting negative conductance of the diode can easily be computed by Gummel-Blue method [26]. From the DC field and current profiles, the spatially dependent ionization rates that appear in the Gummel-Blue equations are evaluated, and fed as input data for the small signal analysis. The edges of the depletion layer of the diode, which are fixed by the dc analysis, are taken as the starting and end points for the small signal analysis. On splitting the diode impedance $Z(x,\omega)$ obtained from Gummel-Blue method, into its real part $R(x,\omega)$ and imaginary part $X(x,\omega)$, two differential equations are framed [26]. A double-iterative simulation scheme incorporating modified Runge-Kutta method is used to solve these two equations simultaneously. The diode negative resistance ($-Z_R$) and reactance ($-Z_X$) are computed through numerical integration of the -R(x) and X (x) profiles over the active space-charge layer. Thus,

$$-Z_R = \int_{-x_1}^{x_2} -R\,dx \text{ and } \quad Z_X = \int_{-x_1}^{x_2} X\,dx \tag{5}$$

The negative conductance (-G), Susceptance (B) and the quality factor (Q_P) of the device can be calculated using the following relations:

$$G = -Z_R / \left(Z_R^2 + Z_X^2\right) \quad \text{and} \quad B = Z_X / \left(Z_R^2 + Z_X^2\right) \tag{6}$$

$$Q_P = -\left(B/G\right)_{\text{at peak frequency}} \tag{7}$$

It may be noted that both –G and B are normalized to the junction area of the diode. The avalanche frequency (f_a) is the frequency at which the imaginary part (B) of the admittance changes its nature from inductive to capacitive. Again it is the minimum frequency at which the real part (−G) of admittance becomes negative and oscillation starts to build up in the circuit.

At a resonant frequency of oscillation, the maximum RF power output (P_{RF}) from the device can be obtained from the following expression,

$$P_{RF} = \frac{1}{2}.V_{RF}^2.\left|-G_p\right|.A \tag{8}$$

where, V_{RF} is the amplitude of the RF swing ($V_{RF} = V_B/2$, assuming 50% modulation of the breakdown voltage V_B), $-G_p$ is the diode negative conductance at the operating frequency and A is the active area (i.e. the junction area) of the diode (10^{-10} m^2). The accuracy of the our method of DC and small-signal simulation of IMPATT devices is increased by incorporating realistic doping profiles, considering recently reported values of material parameter at 300 K [13] and including the effect of mobile space charge [27-29]. The diode negative conductance at the optimum frequency ($-G_p$) is normalized to the area of the diode. The space step for the present simulation technique is set as $\sim 10^{-10}$ m.

The electron and hole current multiplication factors in an unilluminated IMPATT device are given by,

$$M_n = \frac{J_0}{J_{ns(th)}} \text{ and } \quad M_p = \frac{J_0}{J_{ps(th)}} \tag{9}$$

where $J_{ns(th)}$ and $J_{ps(th)}$ are the reverse saturation current densities due to thermally generated electrons and holes respectively. The magnitudes of M_n and M_p are very large ($\geq 10^6$) because $J_{ns(th)}$ and $J_{ps(th)}$ are very small compared to J_0. The current multiplication factors in an IMPATT diode under optically illumination are given by,

$$M_n' = \frac{J_0}{\left\{J_{ns(th)} + J_{ns(opt)}\right\}} \text{ and } \quad M_p' = \frac{J_0}{\left\{J_{ps(th)} + J_{ps(opt)}\right\}} \tag{10}$$

where $J_{ns(opt)}$ and $J_{ps(opt)}$ are respectively the optically generated electron and hole reverse saturation current densities. The photo-generated current will be dominated by holes if the light be incident on the top n^+ substrate of a reverse biased p^+pnn^+ diode. Under this situation the configuration of the diode is known as

Flip-Chip (FC) diode. In this case the value of M_p is considerably reduced (<< 10^6) while M_n remains unchanged (~10^6). The photocurrent will be electron dominated in an illuminated top mounted (TM) structure where the light is incident on the top p^+ surface. In this case the value of M_n is considerably reduced (<< 10^6) while M_p remains unchanged (~10^6). The schematic diagrams of FC and TM DDR IMPATT diode structures under optical illumination are shown in Figure 2. Current distributions inside the top mounted (TM) and flip-chip (FC) DDR IMPATT diodes are shown in Figure 3(a) and Figure 3(b), respectively (where, $J_{ns}' = J_{ns(th)} + J_{ns(opt)}$ and $J_{ps}' = J_{ps(th)} + J_{ps(opt)}$).

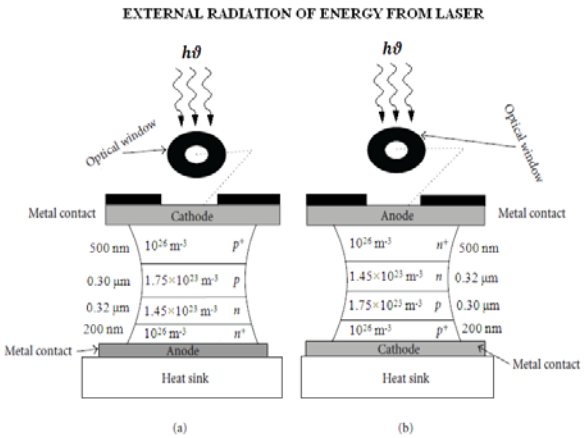

Fig. 2 Schematic diagram of (a) top mounted (TM) and (b) flip chip (FC) DDR IMPATT structures under optical-illumination.

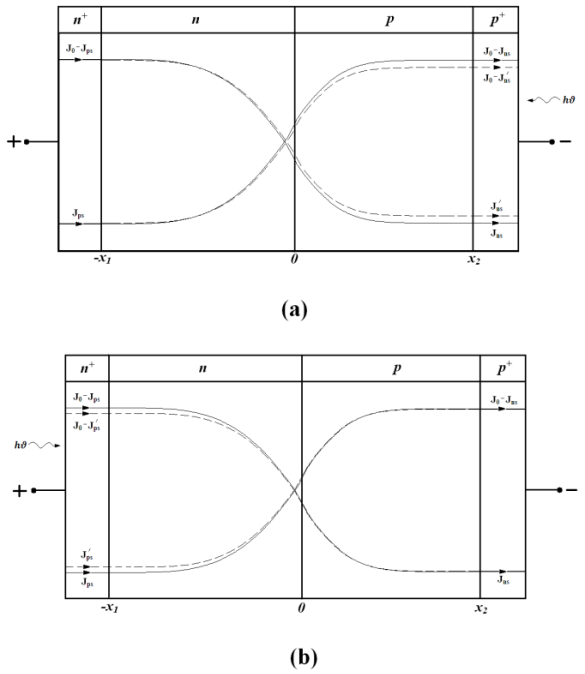

Fig. 3 Current distributions inside the (a) top mounted (TM), (b) flip chip (FC) DDR IMPATT structures.

The boundary conditions in the case of an unilluminated diode are given by equation (2). It can be rewritten as,

$$\left(\frac{J_{diff}}{J_0}\right)_{x=-x_1} = 1 \quad \text{and} \quad \left(\frac{J_{diff}}{J_0}\right)_{x=x_2} = -1 \qquad (11)$$

where $J_{diff} = J_p - J_n$. Because both M_n and M_p are very large (~10^6) in this case. But the boundary condition in the case of an illuminated "FC" diode are given by,

$$\left(\frac{J_{diff}}{J_0}\right)_{x=-x_1} = 1 \quad \text{and} \quad \left(\frac{J_{diff}}{J_0}\right)_{x=x_2} = \left\{\left(\frac{2}{M_p}\right) - 1\right\} \qquad (12)$$

where M_n is very large (~10^6) and M_p is much smaller than M_n. Similarly the boundary condition in the case of an illuminated "TM" diode can be written as,

$$\left(\frac{J_{diff}}{J_0}\right)_{x=-x_1} = \left\{1 - \left(\frac{2}{M_n}\right)\right\} \quad \text{and} \quad \left(\frac{J_{diff}}{J_0}\right)_{x=x_2} = -1 \qquad (13)$$

where M_p is very large (~10^6) and M_n is much smaller than M_p.

The computer simulation methods are used to obtain the R(x) and X(x) profiles in the depletion layer of the illuminated FC and TM diodes for different finite values of M_n and M_p. The computer simulations are carried out for the following diodes,

i) Unilluminated diode ($M_n = 10^6$, $M_p = 10^6$).

ii) Illuminated Flip Chip (FC) diode ($M_n = 10^6$, $M_p << M_n$).

iii) Illuminated Top Mounted (TM) diode ($M_p = 10^6$, $M_n << M_p$).

3 Results and Discussions

A Double Drift Region (DDR) $Si_{0.5}Ge_{0.5}$ (Ge mole fraction, x = 0.5) IMPATT device is designed and optimized to operate at W-Band by using a double iterative, field maximum computer method. The optimized design parameters of the unilluminated $Si_{0.5}Ge_{0.5}$ DDR IMPATT diode for which M_n and M_p are both large (= 10^6) are listed in Table 1. For carrying out a good comparative study a Si based DDR IMPATT diode having the same structural and doping parameters (Table 1) is simulated along with the $Si_{0.5}Ge_{0.5}$ based diode using the simulation technique described in the previous section. Figure 4 shows the doping profile of the diodes used as input of the simulation program. Appropriate exponential and error functions are incorporated into the doping profile to make it realistic. The impact ionization rates, carrier drift velocities and other material parameters for the semiconductor base materials [here Si and $Si_{0.5}Ge_{0.5}$] are taken from published reports [13, 19-22] and incorporated in the analysis.

Table 1 Structural and Doping Parameters of Si and $Si_{0.5}Ge_{0.5}$ DDR IMPATTs.

BASE MATERIAL AND DEVICE STRUCTURE	n-EPITAXIAL LAYER THICNESS (μm)	p-EPITAXIAL LAYER THICNESS (μm)	n-EPITAXIAL LAYER DOPING ($\times10^{23}$ m^{-3})	p-EPITAXIAL LAYER DOPING ($\times10^{23}$ m^{-3})	SUBSTRATE LAYER DOPING ($\times10^{26}$ m^{-3})
Si Flat-DDR	0.3200	0.3000	1.450	1.750	1.0
$Si_{0.5}Ge_{0.5}$ Flat-DDR	0.3200	0.3000	1.450	1.750	1.0

Table 2 Simulated DC and Small-signal Parameters of unilluminated Si and $Si_{0.5}Ge_{0.5}$ DDR IMPATTs.

DIODE STRUCTURE AND BASE MATERIAL	Si DDR	$Si_{0.5}Ge_{0.5}$ DDR
BIAS CURRENT DENSITY, J_0 ($\times10^8$ Amp/m^2)	6.0	6.0
PEAK ELECTRIC FIELD, E_m ($\times10^7$ Volt/m)	6.2375	5.2938
BREAKDOWN VOLTAGE, V_B (Volt)	21.14	18.03
EFFICIENCY, η (%)	9.80	10.87
PEAK OPERATING FREQUENCY, f_p (GHz)	102	97
PEAK CONDUCTANCE, G_P ($\times10^7$ S/m^2)	-6.8122	-6.2264
PEAK SUSCEPTANCE, B_P ($\times10^7$ S/m^2)	12.7882	10.7527
QUALITY FACTOR, $Q_p = (-B_P/G_P)$	1.87	1.73
NEGATIVE RESISTANCE, Z_R ($\times10^{-8}$ Ohm.m^2)	-0.3245	-0.4033
RF POWER OUTPUT, P_{RF} (Watt)	0.3805	0.2530

Table 3 Variation of DC and Small-signal Properties of Si DDR under Optical-Illumination [$J_0 = 6\times10^8$ Amp/m^2].

Optical Illumination Conditions	M_n	M_p	E_m ($\times10^7$ Volt/m)	V_B (Volt)	η (%)	f_p (GHz)	G_P ($\times10^7$ S/m^2)	Q_P	Z_R ($\times10^{-8}$ Ohm.m^2)	P_{RF} (Watt)
Dark	10^6	10^6	6.2375	21.14	9.80	102	-6.8122	1.87	-0.3245	0.3805
Flip Chip	10^6	100	6.2250	21.02	9.52	102.2	-6.7598	1.89	-0.3241	0.3733
	10^6	50	6.2125	20.89	8.89	102.4	-6.3791	1.97	-0.3212	0.3480
Top Mounted	100	10^6	6.2125	20.83	9.11	102.5	-6.3264	1.99	-0.3184	0.3431
	50	10^6	6.2000	20.62	8.49	103	-6.2181	2.05	-0.3097	0.3305

Table 4 Variation of DC and Small-signal Properties of $Si_{0.5}Ge_{0.5}$ DDR under Optical-Illumination [$J_0 = 6\times10^8$ Amp/m^2].

Optical Illumination Conditions	M_n	M_p	E_m ($\times10^7$ Volt/m)	V_B (Volt)	η (%)	f_p (GHz)	G_P ($\times10^7$ S/m^2)	Q_P	Z_R ($\times10^{-8}$ Ohm.m^2)	P_{RF} (Watt)
Dark	10^6	10^6	5.2938	18.03	10.87	97	-6.2264	1.73	-0.4033	0.2530
Flip Chip	10^6	100	5.2875	17.94	10.68	97.7	-6.1042	1.76	-0.4003	0.2456
	10^6	50	5.2872	17.90	10.27	98.2	-6.0529	1.77	-0.3988	0.2424
Top Mounted	100	10^6	5.2873	17.79	10.28	98.1	-5.5521	1.93	-0.3825	0.2196
	50	10^6	5.2750	17.28	9.66	100	-5.1057	2.08	-0.3673	0.1906

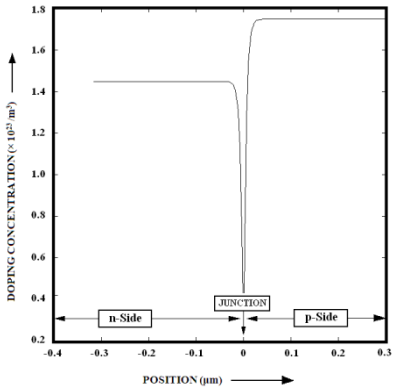

Fig. 4 Doping profile of the diodes.

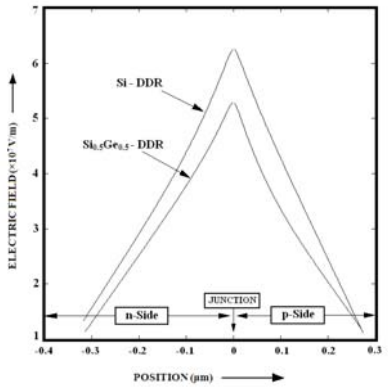

Fig. 5 Electric field profiles of the diodes.

3.1 DC and RF Properties of unilluminated Si and $Si_{0.5}Ge_{0.5}$ DDRs

The DC and high frequency properties of the simulated unilluminated Si and $Si_{0.5}Ge_{0.5}$ DDRs are listed in Table 2 and will be discussed first. Table 2 shows that the W-Band IMPATT device based on $Si_{0.5}Ge_{0.5}$ breaks down at 18.03 Volt. The simulated device ($Si_{0.5}Ge_{0.5}$ DDR) is capable of generating a maximum power output of 253 mW (CW mode) with DC to RF conversion efficiency of 10.87 %, whereas breakdown voltage, CW power output and efficiency of Si based diode are 21.14 Volt, 380 mW and 9.8% respectively. Though the efficiency of the Si DDR is smaller, due to greater avalanche breakdown voltage this diode is capable of giving better RF power output at same bias current density (6×10^8 Amp/m^2). Figure 5 shows the electric field profiles for both the devices. Peak electric field as well as the electric field at every space point within the depletion region of the device is higher for Si DDR than its $Si_{0.5}Ge_{0.5}$ counterpart. Magnitude of Peak negative conductance (Table 2) of Si DDR is larger than that of $Si_{0.5}Ge_{0.5}$ DDR at operating frequency (which is 102 GHz and 97 GHz for unilluminated Si and $Si_{0.5}Ge_{0.5}$ DDRs respectively). But the magnitude of negative resistance is larger for $Si_{0.5}Ge_{0.5}$ DDR at operating frequency. Another noticeable thing is that quality factor at peak operating frequency (Q_p=-B_p/G_p) of $Si_{0.5}Ge_{0.5}$ DDR is less than that of Si DDR. Lesser Q_p means greater stability; which means that stability of $Si_{0.5}Ge_{0.5}$ DDR is better than that of Si DDR.

3.2 Effect of Optical Illumination on Si and $Si_{0.5}Ge_{0.5}$ DDRs

The effects of electron (TM) and hole (FC) dominated photocurrents on the W-Band performance of the Si and $Si_{0.5}Ge_{0.5}$ IMPATTs are presented in Table 3 and Table 4 respectively. The tables show that the magnitudes of negative conductance of the device decrease with the lowering of both M_n and M_p. At the same time, the frequency range over, which the device exhibits negative conductance i.e. the bandwidth of the device, shifts towards higher frequencies with the lowering of both M_n and M_p. The output data for illuminated TM and FC flat structured DDR IMPATT devices indicate that the magnitude of negative conductance at peak frequency $|-G_P|$ decreases by 8.7% when M_n reduces from 10^6 to 50 for Si-based W-Band DDR device, while for the similar lowering of M_p, $|-G_P|$ decreases by 6.4% (Table 3). For the $Si_{0.5}Ge_{0.5}$ DDR the decrements of the same (Table 4) are 17.99% and 2.8% respectively. The identical trend is reflected in Figures 6 and Figure 7, where the admittance plots of Si and $Si_{0.5}Ge_{0.5}$ based photo-illuminated W-Band device are shown. The figures show that the effect of electron dominated photocurrent (TM) in modulating the admittance characteristics is much prominent than the hole dominated photocurrent (FC) for both the devices.

The optimum frequency of oscillation (f_P) for the illuminated Si and $Si_{0.5}Ge_{0.5}$ DDRs increase by 0.98% and 3.1% respectively as M_n reduces from 10^6 to 50. However, for the similar variation of M_p, the upward shift of f_P is much lesser (0.39% and 1.2% respectively). Figures 8 and Figure 9 show the profiles of negative resistivity at the peak frequencies corresponding to different values of M_n and M_p for Si and $Si_{0.5}Ge_{0.5}$ DDRs respectively. Negative resistivity profiles give a physical insight into the region of the depletion layer that contributes to RF power. In each case, the profiles are characterized by two negative resistivity peaks in the middle of the two drift layers of the diode interspaced by a dip in the avalanche region. It is observed from the figures that due to the enhancement of electron and hole photocurrents, the negative resistivity peaks in the electron, and hole drift layers are decreased. It is also found that the decrease in the magnitude of the negative resistivity peaks is more pronounced for variation of M_n corresponding to electron dominated photocurrent (TM) than for the same variation of M_p corresponding to hole dominated photocurrent (FC). Simulation study also depicts that in case of Si and $Si_{0.5}Ge_{0.5}$ based DDR IMPATTs, as M_n is decreased from 10^6 to 50, there occur a 4.6% and 8.9% decrease in the device magnitude of negative resistance ($|-Z_R|$) respectively. On the other hand, as M_p changes from 10^6 to 50, $|-Z_R|$ reduce by 1.02% and 1.11%, respectively (Tables 3 and 4).

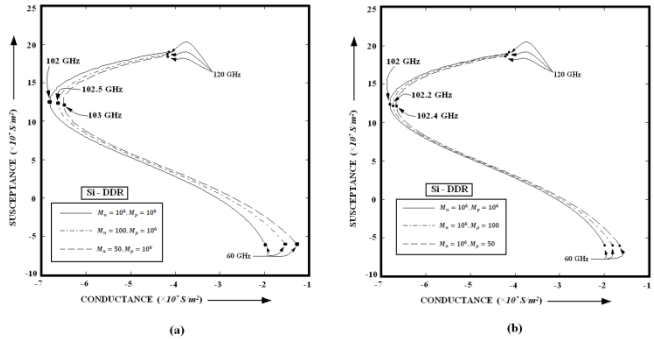

Fig. 6 (a) Effect of electron dominated photo-current (TM), (b) Effect of hole dominated photo-current (FC) on the Admittance Characteristics of the Si based DDR IMPATT device at W-Band.

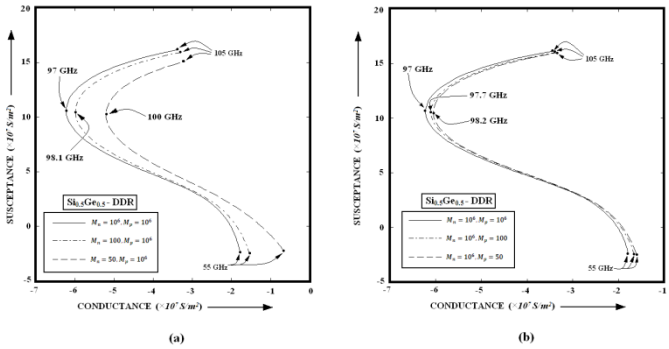

Fig. 7 (a) Effect of electron dominated photo-current (TM), (b) Effect of hole dominated photo-current (FC) on the Admittance Characteristics of the $Si_{0.5}Ge_{0.5}$ based DDR IMPATT device at W-Band.

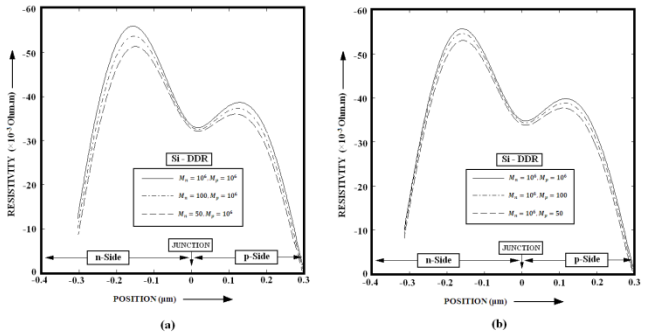

Fig. 8 (a) Effect of electron dominated photo-current (TM), (b) Effect of hole dominated photo-current (FC) on the Negative Resistivity Profiles of the Si based DDR IMPATT device at W-Band.

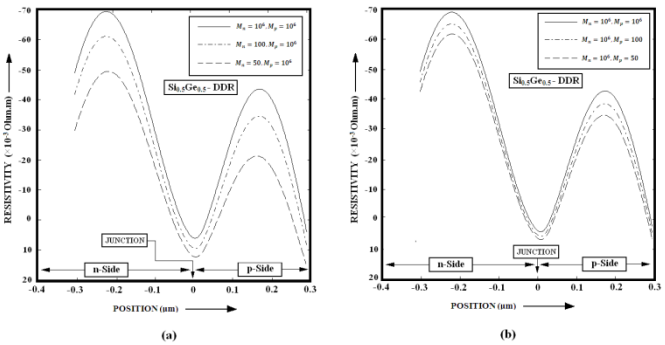

Fig. 9 (a) Effect of electron dominated photo-current (TM), (b) Effect of hole dominated photo-current (FC) on the Negative Resistivity Profiles of the $Si_{0.5}Ge_{0.5}$ based DDR IMPATT device at W-Band.

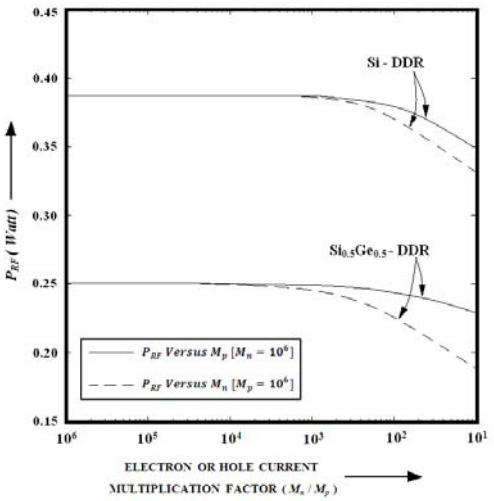

Fig. 10 Effect of electron / hole dominated photo-current on RF Power Output of the Si and $Si_{0.5}Ge_{0.5}$ based DDR IMPATTs at W-Band.

The variations of power output for different values of M_n and M_p are also shown in Table 3 and Table 4. Figure 10 depicts that if M_n is decreased from 10^6 to 10, RF power output for both the diodes decrease more rapidly than if M_p is decreased from 10^6 to 10. Again, it is found from the study that the magnitude of device quality factor at optimum frequency of oscillation (Q_P) increases appreciably for a decrease of M_n compared to the same change of M_p values (Table 3 and Table 4).

3.3 Comparison of Optical Illumination Effect on Si and $Si_{0.5}Ge_{0.5}$ DDRs

The increment of leakage currents by electron and hole dominated photocurrents leads to a decrease of $|-Z_R|$, $|-G_P|$, and P_{RF} along with a simultaneous upward shift of f_P. While the photo-generated leakage current dominated by electrons modifies the DC and high-frequency properties of the device appreciably, that dominated by holes has relatively less effect in modifying the same. This fact can be interpreted on the basis of the relative magnitudes of hole and electron ionization rates in Si and $Si_{0.5}Ge_{0.5}$ for different electric field ranges. The effects of predominant hole and electron photocurrents in FC and TM structures on the avalanche zone width, negative resistance profiles and the admittance characteristics can be explained from the ionization integral,

$$\int_0^{x_A} \left(\alpha_n - \alpha_p\right) dx \qquad (14)$$

where, α_n and α_p are the electron and hole ionization rates and x_A is the width of the avalanche zone. It can be observed from Table 5 the x_A increases with the decrease of M_n and M_p and this increase of x_A is more appreciable in a TM structure than in a FC structure. Further the magnitude of α_n is larger than α_p for the electric field in the avalanche zone of Si and $Si_{0.5}Ge_{0.5}$ based DDRs. Since the above integral (equation 14) depends on x_A and also on $(\alpha_n - \alpha_n)$, the value of the integral would be larger for an TM structure where the electron photocurrent dominates over hole photocurrent than for a FC structure where the situation is just reversed. This explains why the high frequency characteristics of Si and $Si_{0.5}Ge_{0.5}$ DDR oscillators under optical illumination are more sensitive to the photo-generated electron leakage current in a TM structure. But due to the higher values of ionization rates of electrons and holes for $Si_{0.5}Ge_{0.5}$, photo-sensitiveness of $Si_{0.5}Ge_{0.5}$ based DDR is higher than that of Si based DDR, which is one of the major observations of this work.

3.4 Comparison with Experimentally Obtained Results

Experimental results of optically illuminated p^+nn^+ FC and TM structures of silicon IMPATTs show that the electron dominated photo current is more important than the hole dominated photocurrent in modifying the DC & RF properties of silicon IMPATTs [9]. Similar behaviour is observed in the simulation results presented in this paper for optically illuminated p^+pnn^+ FC and TM structures. The tuning of IMPATT oscillators has been demonstrated up to W-Band by Seeds, whereby a 91.83 GHz oscillator was tuned 9.4 MHz with an optically generated current of 20 μA [30]. Whereas the simulation shows about 1 GHz tuning is possible for a 102 GHz Si based DDR IMPATT oscillator under sufficient optical illumination.

Due to lack of experimental data (as per the author's knowledge) on W-Band $Si_{0.5}Ge_{0.5}$ based DDR IMPATT device, the simulation results of $Si_{0.5}Ge_{0.5}$ based DDR could not be compared with experimental results. However, the nature of variation of W-Band properties of the designed diode under photo-illumination has a trend agreement with the experimental results of Si-based IMPATT device at lower frequency region [9, 30]. It may be mentioned here that a large-signal analysis may provide improved quantitative information regarding the influence of optical illumination on the frequency tuning as well as RF power output of the IMPATT device, but the nature of response to optical illumination, as predicted by the small-signal analysis, will remain unaltered.

3.5 Proposed Experimental Setup for Optical Illumination Experiment

An arrangement similar to those shown in Figures 11 and 12 can be used for optical illumination experiment on $Si_{1-x}Ge_x$ IMPATT [8]. The intensity of radiation may be experimentally adjusted by a convex lens as indicated in Figure 11. Bandgap of $Si_{0.5}Ge_{0.5}$ is 0.92 eV, which is corresponding to the wavelength 1.35 μm ($\lambda = hc/E_g$). So an infrared laser source of wavelength 1 μm ($E = hc/\lambda > E_g$; $\lambda = 1$ μm) is sufficient to be used as an optical source for this experiment.

Table 5 Comparison of optical illumination effect on Si and $Si_{0.5}Ge_{0.5}$ based DDR IMPATTs [$J_0 = 6\times10^8$ Amp/m^2].

BASE MATERIAL	DARK			TM			FC		
	$M_n = 10^6$		$M_p = 10^6$	$M_n = 50$		$M_p = 10^6$	$M_n = 10^6$		$M_p = 50$
	x_A (μm)	f_p (GHz)	P_{RF} (mW)	x_A (μm)	f_p (GHz)	P_{RF} (mW)	x_A (μm)	f_p (GHz)	P_{RF} (mW)
Si	0.300	102	380.5	0.314	103	330.5	0.312	102.4	348.0
$Si_{0.5}Ge_{0.5}$	0.298	97	253.0	0.326	100	190.6	0.310	98.2	242.4

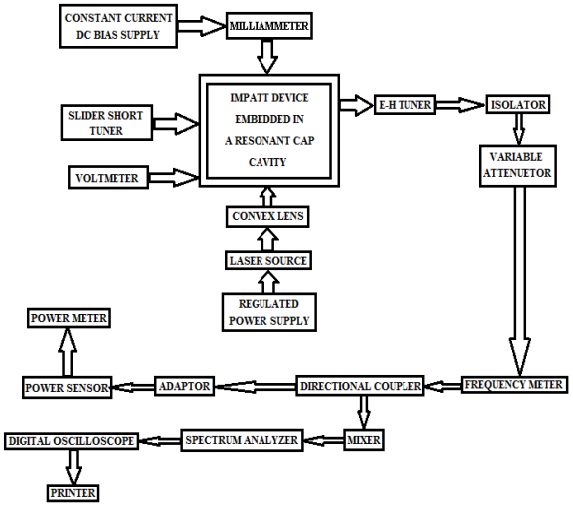

Fig. 11 Experimental setup for optical illumination experiment on $Si_{0.5}Ge_{0.5}$ based DDR IMPATT at W-Band.

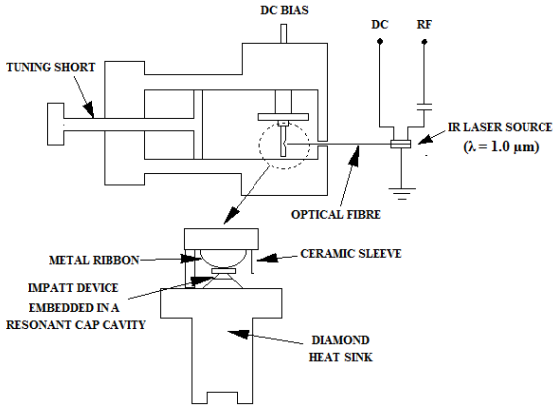

Fig. 12 Resonant Cap Cavity structure for W-Band $Si_{0.5}Ge_{0.5}$ based DDR IMPATT for optical illumination experiment.

4 Conclusions

In this paper the effect of optical illumination on the DC and dynamic properties of Si and $Si_{1-x}Ge_x$ (x = 0.5) based double drift region (DDR) (p^+pnn^+) IMPATT devices operating at W-Band are investigated and compared. It is observed that top mounted structure of both Si and $Si_{0.5}Ge_{0.5}$ based IMPATTs affected more due to optical illumination, i.e. electron dominated photo current effect is prominent for both the devices. But the effect of photon illumination on $Si_{0.5}Ge_{0.5}$ based DDR is more pronounced than Si based DDR; that meant photo-sensitiveness of $Si_{0.5}Ge_{0.5}$ based DDR IMPATT is greater. It is concluded that these findings may be exploited for realizing optically integrated W-Band modules for effective applications in W-Band (75 GHz – 110 GHz) communication and in interstellar explorers.

Acknowledgment

The first author would like to thank Dr. Moumita Mukherjee, Centre of Millimeter wave Semiconductor Devices and Systems, Institute of Radiophysics and Electronics, University of Calcutta for valuable suggestions and helpful discussions.

References

[1] Midford T. A. and Bernick R. L., "Millimeter Wave CW IMPATT diodes and Oscillators", *IEEE Trans. Microwave Theory Tech.*, Vol. 27, No. 5, pp. 483-492, 1979.

[2] Chang Y., Hellum J. M., Paul J. A. and Weller K. P., "Millimeter-Wave IMPATT Sources for Communication Applications", *IEEE MTT-S International Microwave Symposium Digest*, pp. 216-219, 1977.

[3] Gray W. W., Kikushima L., Morentc N. P. and Wagner R. J., "Applying IMPATT Power Sources to Modern Microwave Systems", *IEEE Journal of Solid-State Circuits*, Vol. 4, No. 6, pp. 409-413, 1969.

[4] Mukherjee M. and Roy S. K., "Optically Modulated III–V Nitride-Based Top-Mounted and Flip-Chip IMPATT Oscillators at Terahertz Regime: Studies on the Shift of Avalanche Transit Time Phase Delay Due to Photogenerated Carriers", *IEEE Transactions on Electron Devices*, Vol. 56, No. 7, pp. 1411-1417, 2009.

[5] Banerjee J. P., Mukherjee R., Mukherjee J. and Mallik P. N., "Studies on Avalanche Phase Delay and the Admittance of an Optically Illuminated Indium Phosphide Avalanche Transit Time Diode at Millimeter Wave Window Frequencies", *Phys. Stat. Sol. (a)*, Vol. 153, No. 2, pp. 567-579, 1996.

[6] Seeds A. J. and Augusto A., "Optical control of microwave semiconductor devices", *IEEE trans. on MTT*, Vol. 38, No. 5, pp. 577-585, 1990.

[7] Mukherjee M., Mazumder N. and Dasgupta A., "Analysis of photo-illuminated millimeter wave high power IMPATT oscillator", *in Proceedings*

of the 12th Microcoll Conference on Microwave Communication (MOW '07), Budapest, Hungary, pp. 187-190, 2007.

[8] Mukherjee M., Mazumder N. and Roy S. K., "Prospects of 4H-SiC Double Drift Region IMPATT Device as a Photo-Sensitive High-Power Source at 0.7 Terahertz Frequency Regime", *Active and Passive Electronic Components,* pp. 1-9, 2008.

[9] Vyas H. P., Gutmann R. J. and Borrego J. M., "Effect of hole versus electron photocurrent on microwave-optical interactions in impatt oscillators", *IEEE Transactions on Electron Devices*, Vol. 26, No. 3, pp. 232-234, 1979.

[10] Pei Z., Liang C. S., Lai L. S., Tseng Y. T., Hsu Y. M., Chen P. S., Lu S. C., Liu C. M., Tsai M. J., and Lin C. W., "High efficient 850-nm and 1310-nm multiple quantum well SiGe-Si heterojunction phototransistors with 1.25-plus GHz bandwidth (850 nm)", *IEDM Tech. Dig.*, pp. 297-300, 2002.

[11] Pie Z., Lai L. S., Hwang H. P., Tseng Y. T., Liang C. S. and Tsai M. J., "$Si_{1-x}Ge_x$ multi-quantum well phototransistor for near-infrared operation", *Phys E.*, Vol. 16, No. 3-4, pp. 554-557, 2003.

[12] Pei Z., Liang C. S., Lai L. S., Tseng Y. T., Hsu Y. M., Chen P. S., Lu S. C., Tsai M. J. and Liu C. W., "A high-performance SiGe-Si multiple-quantum well heterojunction phototransistor", *IEEE Electron device letter*, Vol. 24, No. 10, pp. 643-645, 2003.

[13] "Electronic Archive: New Semiconductor Materials, Characteristics and Properties", http://www.ioffe.ru/SVA/NSM/Semicond.

[14] Manku T., McGregor J. M. and Nathan A., "Drift hole mobility in strained and unstrained doped $Si_{1-x}Ge_x$ alloys", *IEEE Transactions on Electron Devices*, Vol. 40, No. 11, pp. 1990-1996, 1992.

[15] Lee J., Gutierrez-Aitken A. L., Li S. H. and Bhattacharya P. K., "Responsivity and impact ionisation Coefficients of $Si_{1-x}Ge_x$ photodiodes", *IEEE Transactions on Electron Devices*, Vol. 43, No. 6, pp. 977-981, 1996.

[16] Roy S. K., Banerjee J. P. and Pati S. P., "Computer methods for the dc field and carrier current profiles in impatt devices starting from the field extremum in the depletion layer", *Proc. of NASECODE-I Conf. on Numerical Analysis of Semiconductor Devices (Dublin: Boole Press)*, pp. 266, 1979.

[17] Roy S. K., Banerjee J. P. and Pati S. P., "A computer analysis of the distribution of high frequency negative resistance in the depletion layers of impatt diodes", *Proc. of NASECODE-IV Conf. on Numerical Analysis of Semiconductor Devices (Dublin: Boole Press)*, pp. 494, 1985.

[18] Sze S. M. and Ryder R. M., "Microwave Avalanche Diodes", *Proc. of IEEE, Special Issue on Microwave Semiconductor Devices*, Vol. 59, No. 8, pp. 1140-1154, 1971.

[19] Canali C., Ottaviani G. and Quaranta A. A., "Drift velocity of electrons and holes and associated anisotropic effects in silicon", *J. Phys. Chem. Solids*, Vol. 32, No. 8, pp. 1707, 1971.

[20] Grant W. N., "Electron and hole ionization rates in epitaxial Silicon", *Solid State Electron*, Vol. 16, No. 10, pp. 1189-1203, 1973.

[21] Ershov M. and Ryzhii V., "High field electron transport in SiGe alloy", *Jpn. J. Appl. Phys*., Vol. 33, No. 3A, pp. 1365-1371, 1994.

[22] Yamada T. and Ferry D. K., "Montecarlo simulation of hole transport in strained $Si_{1-x}Ge_x$", *Solid State Electron*, Vol. 38, No. 4, pp. 881-890, 1995.

[23] Roy S. K., Sridharan M., Ghosh R., and Pal B. B., "Computer method for the dc field and carrier current profiles in the IMPATT device starting from the field extremum in the depletion layer", *in Proceedings of the 1st Conference on Numerical Analysis of Semiconductor Devices (NASECODE I), J. H. Miller, Ed., Dublin, Ireland,* , pp. 266-274, June 1979.

[24] Roy S. K., Banerjee J. P. and Pati S. P., "A Computer analysis of the distribution of high frequency negative resistance in the depletion layer of IMPATT Diodes", *in Proc. 4th Conf. on Num. Anal. of Semiconductor Devices (NASECODE IV) (Dublin) (Dublin: Boole),* pp. 494-500, 1985.

[25] Scharfetter D. L. and Gummel H. K., "Large-Signal Analysis of a Silicon Read Diode Oscillator", *IEEE Trans. on Electron Devices*, Vol. ED 16, No. 1, pp. 64-77, 1969.

[26] Gummel H. K. and Blue J. L., "A small-signal theory of avalanche noise in IMPATT diodes", *IEEE Trans. on Electron Devices*, Vol. ED 14, No. 9, pp. 569-580, 1967.

[27] Gibbons G., *Avalanche-diode microwave oscillators,* Oxford University Press, 1973.

[28] Sridharan M. and Roy S. K., "Computer studies on the widening of the avalanche zone and decrease on efficiency in silicon X-band sym. DDR", *Electron Lett.*, Vol. 14, No. 1, pp. 635-637, 1979.

[29] Sridharan M. and Roy S. K., "Effect of mobile space charge on the small signal admittance of silicon DDR", *Solid State Electron*, Vol. 23, No. 1, pp. 1001-1003, 1980.

[30] Seeds A. J., Singleton J. F., Brunt S. P. and Forrest J. R., "The optical control of IMPATT oscillators", *J. Lightwave Technol.,* Vol. 5, No. 3, pp. 403-411, 1987.

Aritra Acharyya received his M.Tech. degree from Institute of Radiophysics and Electronics, University of Calcutta, Kolkata, W.B., India. Earlier he obtained his B.E. Degree from Bengal Engineering and Science University, Shibpur, Howrah, W.B., India. He worked on Studies on Series Resistance of Millimeter Wave Si-IMPATT Diodes for his Master's thesis, with emphasis on various physical effects like effect of carrier diffusion and tunneling current on series resistance of IMPATT devices. His research interest is millimeter-wave and sub-millimeter-wave semiconductor devices, more specifically IMPATT devices. He is the first author of more than 15 research papers in International and National Journals and conference proceedings.

J. P. Banerjee obtained B.Sc. (Hons.) and M.Sc. in Physics and Ph.D. in Radio Physics and Electronics from University of Calcutta. He worked as a senior scientist of a Department of Electronics project in Institute of Radio Physics and electronics, C.U. during 1986-1989. He joined the Department of Electronic Science, C.U. in 1989 as a reader. He has been working as a professor in the Institute of Radiophysics and Electronics, C.U. since 1998. He is the recipient of Indian National Science Academy Award of a visiting fellowship and Griffith Memorial Prize in Science of the Calcutta University in 1986. He is the principle co-author of more than 150 research papers in International Journals in the fields of Semiconductor Science and Technology, Microwave and Millimeter wave avalanche transit time devices and avalanche Photo Detectors. He has successfully carried out a number of research projects of Government of India on IMPATT devices. A collaborative research work in the field of computer analysis, fabrication and characterization of V-Band silicon double low high low IMPATTs was successfully carried out by Dr. Banerjee for the first time with Dr. J.F. Luy the eminent German Scientist of Daimler Benz research centre. He is a Fellow of Institute of Electronics and Communication Engineers (IETE), a life member of society of EMI and EMC and Semiconductor Society, India. He is an expert committee member of All India Council of Technical Education and served as a referee for various technical journals.